3
Flow with Particles

The flow with particles is solved in the same fashion as the flow without particles. However, new equations and unknowns arise. The Continuity Equation (2.4) remains the same, but the Momentum Equations are augmented with a new variable, a vector field of Lagrange Multipliers $\overrightarrow{\lambda}$. Besides the Lagrange Multipliers, the translational and angular velocities of the particles are new variables introduced and each of them brings a new equation to be solved.

In this chapter we will discuss the formulation of the problem with the new variables and respective equations. First we will present the idea of Fictitious Domain (19), which is closely related to the introduction of the field $\overrightarrow{\lambda}$. Then we will discuss the Rigid Body Dynamics equations that govern the mechanics of the spherical particles.

Before we present formulation of the problem, we first shall present the nomenclature used to deal with the domains. This work studies the flow of one phase of fluid with as many particles as desired – of course the number of particles if bounded by the computational resources, i.e. memory and processor speed. The entire domain is referred by Ω, the fluid phase by Ω_f and the Particle k by Ω_{P_k}. Figure 3.1 displays these domains, where $\Omega = \Omega_f \bigcup \Omega_{P_k}$.

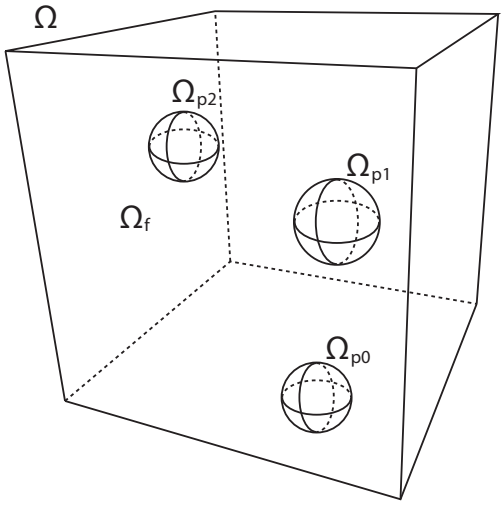

Figure 3.1: The entire domain Ω, the fluid domain Ω_f and three particles Ω_{P_k}.

3.1 Fictitious Domain Method

The most natural way to think about the problem of flows with particles is to generate a mesh in the fluid domain that wraps around each particle in order to solve the Navier-Stokes equations inside the fluid domain and the Rigid Body equations inside the particle domain. However, this approach may be expensive computationally . At every time step a new mesh would have to be generated as depicted in figure 3.2. To avoid this cost, the Fictitious Domain Method is employed in this work.

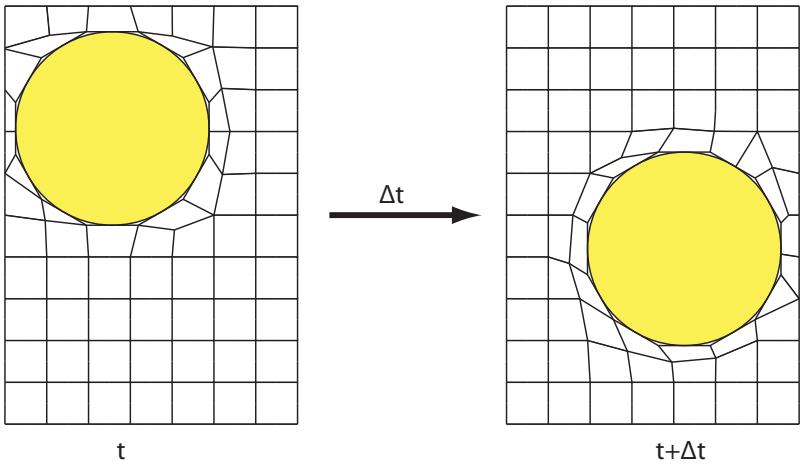

Figure 3.2: Mesh wrapping around the particle.

Fictitious domain method was introduced by Hyman (19) and its main idea is to extend a geometrically complex and possibly time-dependent domain to a larger and simpler one. In this work, the fluid domain is geometrically complex because of the holes produced by the particles. Besides, these holes move along time following the particles' paths, what makes the domain time-dependent. The simpler domain consists of the domain comprised by fluid and particles. This extended domain needs to be discretized only once, as it is time-independent, see fig. 3.3. The particles move inside the domain, and do not change its shape. Besides, as it is simpler, regular meshes can be employed. The boundary conditions of the original domain must be enforced in the extended domain, so that the solutions of the problem on the extended and original domains match each other.

The first works using fictitious domain method to simulate flows interacting with particles were proposed by Glowinski et al. (15, 14). In these works, the particles had prescribed motions. Later, Glowinski et al. (16) proposed a formulation to take into account the motion of the particles imposed by hydrodynamic force and torque.

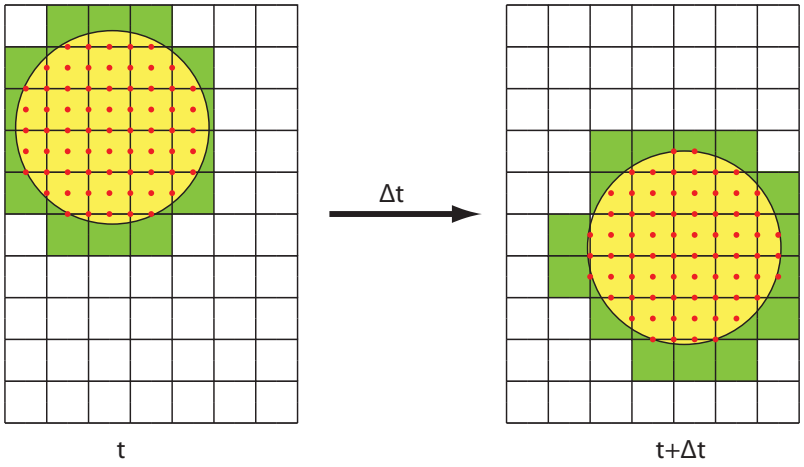

Figure 3.3: Fixed mesh at every instant of time.

The formulation used in this work follows the one presented by Lage (21) with a slight difference on the momentum equations. The computation of the laplacian of the $\overrightarrow{\lambda}$ field in the augumented momentum conservation is not simplified as done in Lage's thesis. We chose to do so, as it is not expensive to compute the laplacian in the variational form. Lage's formulation modifies a previous formulation proposed by Diaz-Goano et al (12). In Diaz-Goano et al., the particle's weight is written as the particle's relative weight, what causes a double computation of the buoyancy force. In Lage's thesis, the absolute weight is used and the double computation of buoyancy is avoided. Thus, unphysical behavior is avoided.

3.2 Formulation of flows with suspended particles

Consider the velocity field $\overrightarrow{V_p}$ as a rigid body velocity field inside the particles and zero in the fluid:

$$\overrightarrow{V_P} = \begin{cases} \overrightarrow{V_{P_k}} + \overrightarrow{\omega_{P_k}} \times (\overrightarrow{x} - \overrightarrow{X_{P_k}}) & \text{in } \Omega_{P_k} \\ 0 & \text{in } \Omega_f \end{cases} \tag{3.1}$$

The integral momentum equation for $\overrightarrow{V_P}$ inside Ω_{P_k} follows:

$$\int_{\Omega_{P_k}} \rho_{P_k} \frac{D\overrightarrow{V_{P_k}}}{Dt} d\Omega_{P_k} = \int_{\Omega_{P_k}} \rho_{P_k} \overrightarrow{g}\, d\Omega_{P_k} + \int_{\partial\Omega_{P_k}} \overrightarrow{n_{P_k}} \cdot \boldsymbol{\sigma_f} d\partial\Omega_{P_k} \tag{3.2}$$

where $\overrightarrow{n_{P_k}}$ is the normal vector on the particle surface pointing outward the particle. The last integral is an integral over the particle P_k surface. It computes the total hydrodynamic force and torque acting on the particle.

The stress tensor of the fluid $\boldsymbol{\sigma_f}$ can be extended over the entire domainΩ.

Thus we have:

$$\boldsymbol{\sigma} = -p\boldsymbol{I} + \mu\left[\left(\overrightarrow{\nabla}\overrightarrow{V}\right) + \left(\overrightarrow{\nabla}\overrightarrow{V}\right)^T\right]$$

Equation 3.2 can be rewritten using this tensor and applying the divergence theorem and we get

$$\int_{\Omega_{P_k}} \rho_{P_k}\frac{D\overrightarrow{V_{P_k}}}{Dt}d\Omega_{P_k} = \int_{\Omega_{P_k}} \rho_{P_k}\overrightarrow{g}\,d\Omega_{P_k} + \int_{\Omega_{P_k}} \overrightarrow{\nabla}\cdot\boldsymbol{\sigma}\,d\Omega_{P_k} \tag{3.3}$$

Defining a force $\overrightarrow{F}$ per volume unit

$$\overrightarrow{F} = \begin{cases} -\rho_f\dfrac{D\overrightarrow{V}}{Dt} + \mu\overrightarrow{\nabla}\overrightarrow{V} & \text{in } \Omega_{P_k} \\ 0 & \text{in } \Omega_f \end{cases} \tag{3.4}$$

and adding a constraint to the extended velocity field $\overrightarrow{V}$ that enforces $\overrightarrow{V} = \overrightarrow{V_P}$ in Ω_{P_k}, we end up with the following equation for the momentum of the particle P_k:

$$\int_{\Omega_{P_k}} (\rho_{P_k} - \rho_f)\frac{D\overrightarrow{V}}{Dt}d\Omega_{P_k} = \int_{\Omega_{P_k}} \rho_{P_k}\overrightarrow{g} - \overrightarrow{\nabla}p + \overrightarrow{F}\,d\Omega_{P_k} \tag{3.5}$$

As discussed in more details in Lage (21), $\overrightarrow{F}$ avoids viscous deformation inside the particles. Thus, it enforces a rigid body velocity field inside the particle domain.

Keeping in mind that, inside the particle P_k, $\overrightarrow{V} = \overrightarrow{V_{P_k}} + \overrightarrow{\omega_{P_k}}\times(\overrightarrow{x} - \overrightarrow{X_{P_k}})$, we can write the material derivative inside the particle P_k as:

$$\frac{D\overrightarrow{V}}{Dt} = \frac{D}{Dt}\left(\overrightarrow{V_{P_k}} + \overrightarrow{\omega_{P_k}}\times(\overrightarrow{x} - \overrightarrow{X_{P_k}})\right) = \frac{\partial}{\partial t}\left(\overrightarrow{V_{P_k}} + \overrightarrow{\omega_{P_k}}\times(\overrightarrow{x} - \overrightarrow{X_{P_k}})\right) \tag{3.6}$$

If we substitute $D\overrightarrow{V}/Dt$ on eq.3.5 by the last term of eq.3.6, we obtain

$$\int_{\Omega_{P_k}} (\rho_{P_k} - \rho_f)\frac{\partial\overrightarrow{V}}{\partial t}d\Omega_{P_k} + \int_{\Omega_{P_k}} (\rho_{P_k} - \rho_f)\frac{\partial}{\partial t}\left(\overrightarrow{\omega_{P_k}}\times(\overrightarrow{x} - \overrightarrow{X_{P_k}})\right)d\Omega_{P_k} = \int_{\Omega_{P_k}} \rho_{P_k}\overrightarrow{g} - \overrightarrow{\nabla}p + \overrightarrow{F}\,d\Omega_{P_k} \tag{3.7}$$

Observe that the volume of the particle is constant along time, the particle is perfectly spherical and $\overrightarrow{X_{P_k}}$ lies at the center of the sphere. Thus, we can change the order between the time derivative and the integration operators in equation 3.7. It gives the following equation:

$$\frac{\partial}{\partial t}\int_{\Omega_{P_k}} (\rho_{P_k} - \rho_f)\left(\overrightarrow{\omega_{P_k}}\times(\overrightarrow{x} - \overrightarrow{X_{P_k}})\right)d\Omega_{P_k} = 0 \tag{3.8}$$

Taking 3.8, we can rewrite 3.7 and we get the final equation for the particle P_k's velocity $\overrightarrow{V_{P_k}}$:

$$\int_{\Omega_{P_k}} (\rho_{P_k} - \rho_f)\frac{\partial \overrightarrow{V}}{\partial t} d\Omega_{P_k} = \int_{\Omega_{P_k}} \rho_{P_k} \overrightarrow{g} - \overrightarrow{\nabla} p + \overrightarrow{F} d\Omega_{P_k} \tag{3.9}$$

Angular velocity $\overrightarrow{\omega_{P_k}}$ can be recovered assuming the no-slip boundary condition on the particle's interface $\partial\Omega P_k$.

$$\overrightarrow{\omega_{P_k}} \times \left(\overrightarrow{x} - \overrightarrow{X_{P_k}}\right) = \left(\overrightarrow{V} - \overrightarrow{V_{P_k}}\right) \text{ in } \partial\Omega_{P_k}$$

then, we can integrate over the particle's surface to get

$$\int_{\partial\Omega_{P_k}} \overrightarrow{\omega_{P_k}} \times \left(\overrightarrow{x} - \overrightarrow{X_{P_k}}\right) \cdot \overrightarrow{n_{P_k}} ds = \int_{\partial\Omega_{P_k}} \left(\overrightarrow{V} - \overrightarrow{V_{P_k}}\right) \cdot \overrightarrow{n_{P_k}} ds$$

The final equation for the angular velocity is obtained considering the properties of the curl operator and Stokes' theorem. Se we can write:

$$\int_{\Omega_{P_k}} \overrightarrow{\omega_{P_k}} d\Omega_{P_k} = \frac{1}{2} \int_{\Omega_{P_k}} \overrightarrow{\nabla} \times \left(\overrightarrow{V} - \overrightarrow{V_{P_k}}\right) d\Omega_{P_k} \tag{3.10}$$

The momentum equation for the fluid phase can be written in terms of the extended velocity $\overrightarrow{V}$ and pressure p fields and stress tensor $\boldsymbol{\sigma}$ with the fictitious force $\overrightarrow{F}$:

$$\rho_f \frac{D\overrightarrow{V}}{Dt} = \overrightarrow{\nabla} \cdot \boldsymbol{\sigma} + \rho_f \overrightarrow{g} - \overrightarrow{F} \text{ in } \Omega \tag{3.11}$$

Substituting the definition of the fictitious force $\overrightarrow{F}$ onto eq.3.11 for the particle P_k domain Ω_{P_k}, we can see that it reduces to the definition of the buoyancy force acting on the particle:

$$\int_{\Omega_{P_k}} \nabla p \, d\Omega_{P_k} = \int_{\Omega_{P_k}} \rho_f \overrightarrow{g} \, d\Omega_{P_k} \tag{3.12}$$

Now we can define a global Lagrange multiplier $\overrightarrow{\lambda}$ that is related to $\overrightarrow{F}$, as in Lage (21) and Diaz-Goano et al. (12). The definition of $\overrightarrow{\lambda}$ follows the boundary value problem:

$$\overrightarrow{F} = -\alpha \overrightarrow{\lambda} + \mu \overrightarrow{\nabla}^2 \overrightarrow{\lambda} \qquad \text{in } \Omega \tag{3.13a}$$

$$\overrightarrow{\lambda} = \overrightarrow{0} \qquad \text{on } \partial\Omega \tag{3.13b}$$

where α is a positive constant. Following the discussions on Diaz-Goano et al.

(12), we used

$$\alpha = \frac{3\rho_f}{2\Delta t}$$

Equations 3.13a and 3.13b define a well posed problem for $\overrightarrow{F} \in \mathbb{L}^2$ as discussed in Diaz-Goano et al. (12). Thus, we have the complete formulation of the flow with suspended particles using fictitious domain method:

$$\rho_f \frac{D\overrightarrow{V}}{Dt} = \overrightarrow{\nabla} \cdot \sigma + \rho_f \overrightarrow{g} + \alpha \overrightarrow{\lambda} - \mu \overrightarrow{\nabla}^2 \overrightarrow{\lambda} \quad \text{in } \Omega \tag{3.14a}$$

$$\overrightarrow{\nabla} \cdot V = \overrightarrow{0} \quad \text{in } \Omega \tag{3.14b}$$

$$\int_{\Omega_{P_k}} (\rho_{P_k} - \rho_f) \frac{\partial \overrightarrow{V_{P_k}}}{\partial t} d\Omega_{P_k} = \int_{\Omega_{P_k}} \rho_{P_k} \overrightarrow{g} - \overrightarrow{\nabla} p - \alpha \overrightarrow{\lambda} + \mu \overrightarrow{\nabla}^2 \lambda \, d\Omega_{P_k} \quad \text{in } \Omega_{P_k} \tag{3.14c}$$

$$\int_{\Omega_{P_k}} \overrightarrow{\omega_{P_k}} \, d\Omega_{P_k} = \frac{1}{2} \int_{\Omega_{P_k}} \overrightarrow{\nabla} \times \left(\overrightarrow{V} - \overrightarrow{V_{P_k}} \right) d\Omega_{P_k} \quad \text{in } \Omega_{P_k} \tag{3.14d}$$

Besides the system of equations 3.14, the the ridig body constraint, the Lagrange multipliers and the particle advection equations must be included in the complete formulation:

$$\overrightarrow{\lambda} = \overrightarrow{0} \quad \text{in } \Omega_f \tag{3.15a}$$

$$\overrightarrow{V} = \overrightarrow{V_{P_k}} + \overrightarrow{\omega_{P_k}} \times (\overrightarrow{x} - \overrightarrow{X_{P_k}}) \quad \text{in } \Omega_{P_k} \tag{3.15b}$$

$$\frac{\partial \overrightarrow{X_{P_k}}}{\partial t} = \overrightarrow{V_{P_k}} \quad \forall P_k \tag{3.15c}$$

3.3 Variational Formulation

To solve the system of equations 3.14 and 3.15 with Finite Element Method, we may write them in a variational form. The choice for the solution space of the fluid's velocity and pressure, the Lagrange multipliers field and the particles' velocities is:

$$\mathbb{C} = \{(\overrightarrow{V}, p, \overrightarrow{\lambda}, \overrightarrow{V_{P_k}}, \overrightarrow{\omega_{P_k}}) | \overrightarrow{V} \in \mathbb{V}, p \in \mathbb{P}, \overrightarrow{\lambda} \in \mathbb{L}, \overrightarrow{V_{P_k}} \in \mathbb{R}^3, \overrightarrow{\omega_{P_k}} \in \mathbb{R}^3\}$$

where $P_k \in (0, 1, 2, ..., n_p - 1)$ and the spaces $\mathbb{V}$, $\mathbb{P}$ and $\mathbb{L}$ are defined as:

$$\mathbb{V} := \{\overrightarrow{V} \in \mathbb{H}^1(\Omega) | \overrightarrow{V}|_{\partial\Omega} = \overrightarrow{0}\}$$
$$\mathbb{L} := \{\overrightarrow{\lambda} \in \mathbb{H}^1(\Omega) | \overrightarrow{\lambda}|_{\Omega_f} = \overrightarrow{0}\}$$
$$\mathbb{P} := \{p \in \mathbb{H}^0(\Omega)\}$$

As in Lage (21), to extend the formulation over the entire domain, we remove the fluid's velocity restriction inside the particles $\overrightarrow{V} = \overrightarrow{V_{P_k}} + \overrightarrow{\omega_{P_k}} \times (\overrightarrow{x} - \overrightarrow{X_{P_k}})$ fro the combined solution space and enforce it as a side constraint. As is was presented before, this is done by mean of the $\overrightarrow{\lambda}$ field, which is non-zero only inside the particles and enforces this rigid body velocity field inside them.

Equation 3.14d, the one for $\overrightarrow{\omega_{P_k}}$ is used without any further manipulation. The one for the particles' velocity $\overrightarrow{V_{P_k}}$, eq. 3.14c, will be manipulated using the divergence theorem in the Laplacian of $\overrightarrow{\lambda}$:

$$\int_{\Omega_{P_k}} (\rho_{P_k} - \rho_f) \frac{\partial \overrightarrow{V_{P_k}}}{\partial t} \, d\Omega_{P_k} = \int_{\Omega_{P_k}} \rho_{P_k} \overrightarrow{g} - \overrightarrow{\nabla} p - \alpha \overrightarrow{\lambda} \, d\Omega_{P_k} + \int_{\partial\Omega_{P_k}} \mu \overrightarrow{\nabla} \overrightarrow{\lambda} \cdot \overrightarrow{n_{P_k}} \, d\partial\Omega_{P_k} \tag{3.16}$$

The variational formulation of the problem of flow with suspended particles is finally presented: Find $\overrightarrow{V} \in \mathbb{V}$, $p \in \mathbb{P}$, $\overrightarrow{\lambda} \in \mathbb{L}$, $\overrightarrow{V_{P_k}} \in \mathbb{R}^3$ and $\overrightarrow{\omega_{P_k}} \in \mathbb{R}^3$ such that $\forall \overrightarrow{\phi} \in \mathbb{H}^1(\Omega)$ and $\forall \psi \in \mathbb{H}^0(\Omega)$:

$$\int_{\Omega} \rho_f \left(\frac{D\overrightarrow{V}}{Dt} - \overrightarrow{g} \right) \cdot \overrightarrow{\phi} \, d\Omega = \int_{\Omega} \alpha \overrightarrow{\lambda} \cdot \overrightarrow{\phi} - \boldsymbol{\sigma} : \overrightarrow{\nabla} \overrightarrow{\phi} + \mu \overrightarrow{\nabla} \overrightarrow{\lambda} : \overrightarrow{\nabla} \overrightarrow{\phi} \, d\Omega \qquad \text{in } \Omega \tag{3.17a}$$

$$\int_{\Omega} \left(\overrightarrow{\nabla} \cdot \overrightarrow{V} \right) \psi \, d\Omega = 0 \qquad \text{in } \Omega \tag{3.17b}$$

$$\int_{\Omega_{P_k}} (\rho_{P_k} - \rho_f) \frac{\partial \overrightarrow{V_{P_k}}}{\partial t} \, d\Omega_{P_k} = \int_{\Omega_{P_k}} \rho_{P_k} \overrightarrow{g} - \overrightarrow{\nabla} p - \alpha \overrightarrow{\lambda} \, d\Omega_{P_k} \qquad \text{in } \Omega_{P_k} \tag{3.17c}$$

$$\int_{\Omega_{P_k}} \overrightarrow{\omega_{P_k}} \, d\Omega_{P_k} = \int_{\Omega_{P_k}} \overrightarrow{\nabla} \times \left(\overrightarrow{V} - \overrightarrow{V_{P_k}} \right) d\Omega_{P_k} \qquad \text{in } \Omega_{P_k} \tag{3.17d}$$

The reader may notice that the integral over the boundaries of the particles $\partial\Omega_{P_k}$ were removed from equation 3.17c. This integral was neglected, because the particles' boundary are not explicitly represented in our approach

(21). Besides the system of equatinos 3.17, we must include the rigid body constraint for the velocity field inside the particles and the Lagrange multipliers equations. We must also include the particle's advection:

$$\int_{\Omega_f} \overrightarrow{\lambda} \cdot \overrightarrow{\phi}\, d\Omega_f = \overrightarrow{0} \qquad \text{in } \Omega_f \tag{3.18a}$$

$$\int_{\Omega_{P_k}} \left(\overrightarrow{V} - \overrightarrow{V_{P_k}}\right) \cdot \overrightarrow{\phi}\, d\Omega_{P_k} = \int_{\Omega_{P_k}} \omega_{P_k} \times \left(\overrightarrow{x} - \overrightarrow{X_{P_k}}\right) \cdot \overrightarrow{\phi}\, d\Omega_{P_k} \qquad \text{in } \Omega_{P_k} \tag{3.18b}$$

$$\frac{\partial \overrightarrow{X_{P_k}}}{\partial t} = \overrightarrow{V_{P_k}} \qquad \forall P_k \tag{3.18c}$$

All these equations are presented component-wise in appendix B. Also their respective residues and Jacobian entries are there for further detail.

The positions of the particles are integrated over time using Euler integration, such that:

$$\frac{\partial \overrightarrow{X_{P_k}}}{\partial t} = \overrightarrow{V_{Pk}} \tag{3.19}$$

For the sake of animation, we kept track of the rotation of the particles. While the position suffered translation, the local axis of the particles suffered rotation. We defined the local axis as an orthonormal basis in $\mathbb{R}^3$ with the vectors $\hat{e}_{xP_k}$,$\hat{e}_{yP_k}$ and $\hat{e}_{zP_k}$. The rotation is applied with the angular velocity tensor (5). In this work, we rotated the vectors $\hat{e}_{\star P_k}$ as follows:

$$\frac{\partial \hat{e}_{\star P_k}}{\partial t} = \overrightarrow{\omega_{P_k}} \times \hat{e}_{\star P_k} \tag{3.20}$$

After the rotations, the basis was re-orthogonalized and the vectors normalized. As the angles of rotation are important only for animation purpose, we did not care about precision. Otherwise we would use quaternions, instead.

3.3.1 The Elementary Degrees of Freedom

Each element, as seen before, is comprised by 27 nodes. Now, each node has 6 DOFs. Besides the DOFs of velocity, they also have the DOFs of Lagrange Multipliers λ_x, λ_y and λ_z.

3.4 Validation

One of the tests we have performed to validate the code was to check if an initial guess could satisfy the solution. To do so, we used the ρ_{Pk} equal to ρ_f and set the pressure field to the hydrostatic pressure. The solution for this problem, with all 6 walls at rest, is no movement at all and the pressure field is the hydrostatic pressure itself. Our results showed that the residue computed for these data results in a value as low as 3.52×10^{-12}, as expected. We used the 2-norm for the residuals vector.

Also, for the same problem, we initialized the pressure field with zeros. The solution converged to no movement and the pressure field equal to the hydrostatic pressure field. The zero pressure level is the y coordinate of the center node in the first element. This is the element where we reference the pressure level equal to zero.

3.5 Results

3.5.1 Sedimenting Particle

We simulated the 3D flow of a sedimenting particle (P) inside a cavity with a mesh $8 \times 16 \times 8$. The cavity dimensions were $1.0 \times 2.0 \times 1.0$. The parameters were set as follows:

$$\begin{aligned} \rho_f &= 1.0 \\ \mu &= 1.0 \\ \rho_P &= 1.5 \\ R_P &= 0.2 \\ \overrightarrow{g} &= [0, -10, 0]^T \end{aligned}$$

where ρ_P is the specific mass of the particle and R_P is its radius. The initial position was $[0, 1, 0]^T$ and the domain range was $x \in [-0.5, 0.5]$, $y \in [-0.5, 1.5]$ and $z \in [-0.5, 0.5]$.

The boundary conditions in all 6 walls were of no-slip and their velocities were zero ($\overrightarrow{0}$). The velocity, Lagrange Multipliers and pressure fields were initially zero and the particle at rest. In the first time step ($0.1s$), we obtained the velocity and λ fields displayed in figs. 3.5 and 3.6.

$0-26$	$27-53$	$54-80$	$81-84$	$85-111$	$112-138$	$139-165$
u	v	w	P	λ_x	λ_y	λ_z

Table 3.1: The elemental degrees of freedom and its indexation for particulate flow.

The particle position on the domain at $0.1s$ and the mesh are displayed in fig. 3.4.

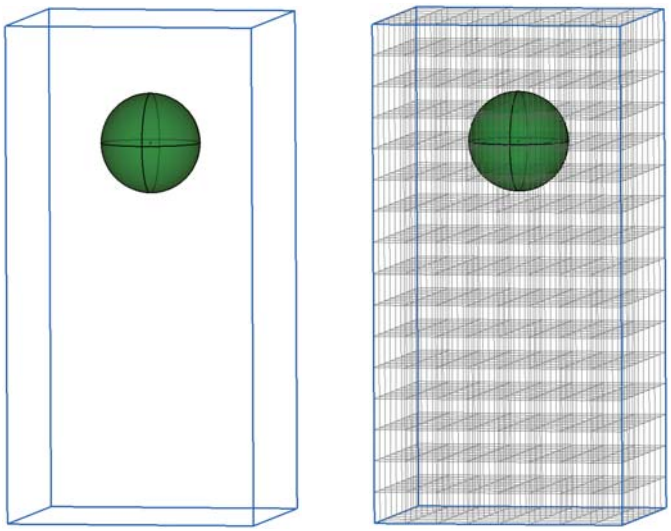

3.4(a): Particle in 3D space 3.4(b): Mesh in 3D space

Figure 3.4: The sedimenting particle and the mesh used to simulate the flow.

The pressure field on the mid z plane at $0.1s$ is displayed in figure 3.7. Observe how the pressure field is the hydrostatic pressure field.

The simulation ran until a point at which Newton's method did not converge. It happened around the time instant of $70s$. Until this instant, we plotted the evolution in time of position and velocity components of the particle. These plots are presented in figs. 3.8, 3.9 and 3.10. Observe that the variation of the position y component is higher than that of x and z, indicating the tendency of the particle to fall on the direction of the gravity $\overrightarrow{g}$ field as expected. The abrupt change in the variation can be noticed and it happens when the movement of the particle causes it change the number of Gauss points used in the numerical integration required. As the particle moves through the mesh, some nodes (and Gaussian points) get in and outside the particle. When this happens, the integration domain of the equations changes abruptly and causes the fluctuation. With a refined mesh, the fluctuation can be negligible. However, with our coarse meshes, these fluctuations cannot be negligible as we desired. See Lage (21) about this discussion.

The same effect of the mesh can be seen on the linear velocity (fig. 3.9) and angular velocity (fig. 3.10). The reader may notice how the linear velocity y component is much higher than the other coordinates, as discussed for the position variation. The angular velocity has some variations. However, they oscillate around zero with a low absolute value

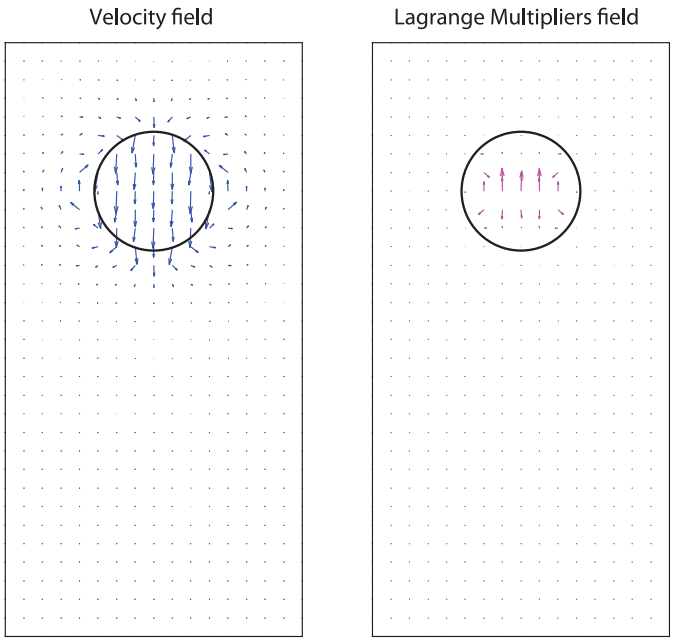

3.5(a): Velocity field on the vertical plane.

3.5(b): Lagrange Multipliers field on the vertical plane.

Figure 3.5: Velocity and Lagrange Multipliers fields on the plane $z = 0$ of the 3D flow with one particle. Notice the rigid body motion inside the particle and that λ is zero in the fluid domain.

3.5.2 Flow with Particle in a 3D Lid-Driven Cavity

Besides the sedimenting particle results, we obtained results of a particulate flow in a 3D lid-driven cavity. The ρ_P was set with the same value of ρ_f in order to see the influence of the flow on the particle, minimizing the effects of gravity against buoyancy. The mesh used was $10 \times 10 \times 10$. The simulation ran up to $0.6s$. After that instant of time, the Newton Method did not converge due to mesh inaccuracy. The position variation of the particle against time, as well as its linear and angular velocities are displayed in figures 3.12, 3.13 and 3.14. The parameters were adjusted as follows:

$$\begin{aligned} \rho_f &= 1.0 \\ \mu &= 0.1 \\ \rho_P &= 1.0 \\ R_P &= 0.1 \\ \overrightarrow{g} &= [0, -10, 0]^T \\ u_l &= 1.0 \end{aligned}$$

The Newton Method does not converge at 0.6 seconds and we believe that it is because, once the mesh does not discretize well the particle, some

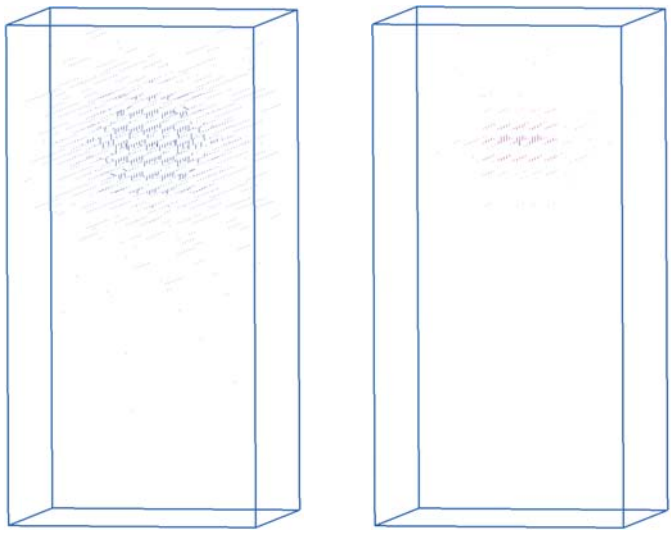

3.6(a): Velocity field on 3D space.

3.6(b): Lagrange Multipliers field on 3d space.

Figure 3.6: Velocity and Lagrange Multipliers fields of the 3D flow with one particle. Notice the rigid body motion inside the particle on the velocity field and that λ is zero in the fluid domain.

portions of it are neglected in the integration. The integration is performed by Gaussian Quadrature. In elements with at least one particle, we used 7 Gauss points –in each direction– and in the ones without particles, we used 3. The numbers of Gaussian points are, in 3D, respectively 49 and 9. Results with 7 points have proven to be better than the ones with 3 points. So we use 7. We also tried 10 points, however the results were worse than with 7. The initial position of the particle in the cavity is presented in figure 3.11. This position was $[0, 0, 0]^T$ and the domain range was $x \in [-0.5, 0.5]$, $y \in [-0.5, 0.5]$ and $z \in [-0.5, 0.5]$ – a cube.

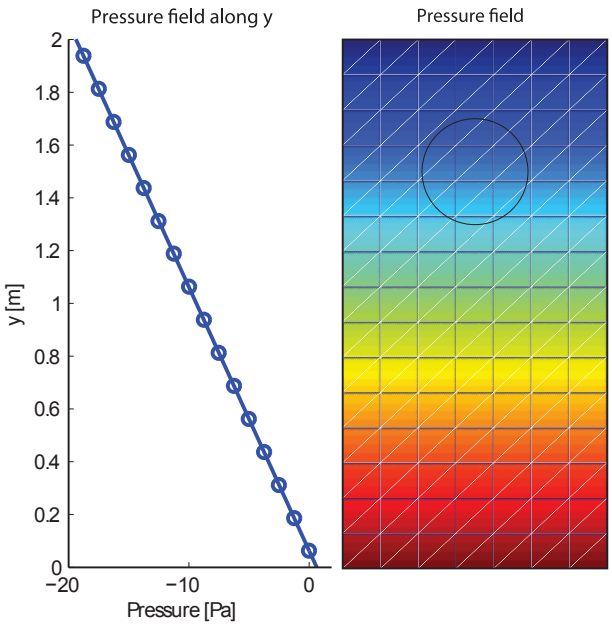

Figure 3.7: Pressure field obtained on the instant 0.1s.

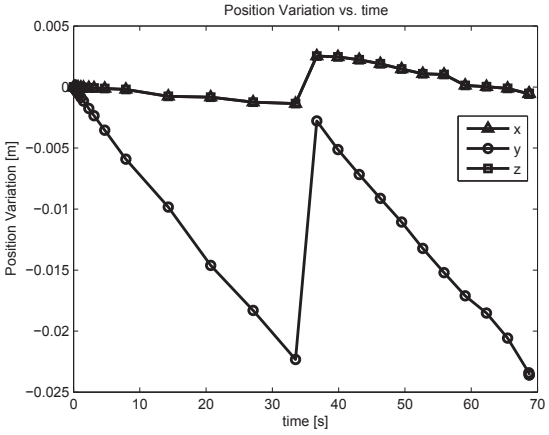

Figure 3.8: Position variation components (x, y, z) of the sedimenting particle against time.

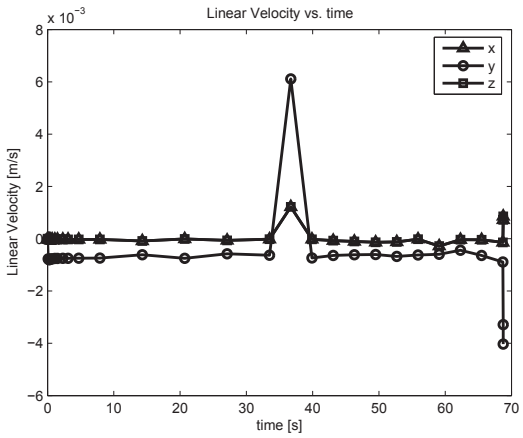

Figure 3.9: Linear velocity components (x, y, z) of the sedimenting particle against time.

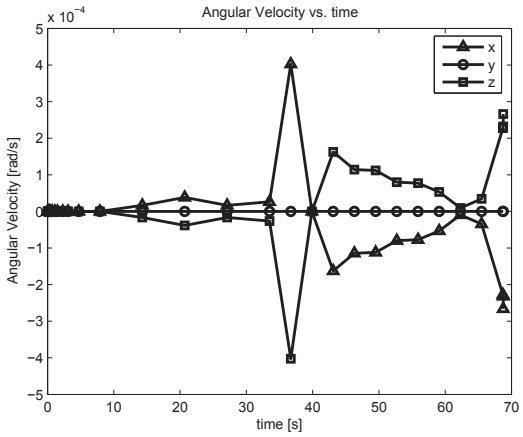

Figure 3.10: Angular velocity components (x, y, z) of the sedimenting particle against time.

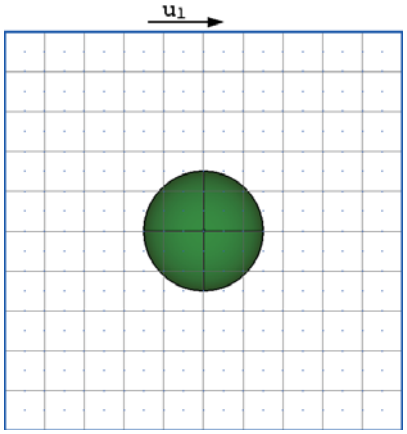

Figure 3.11: Initial configuration of the lid-driven cavity flow with a particle.

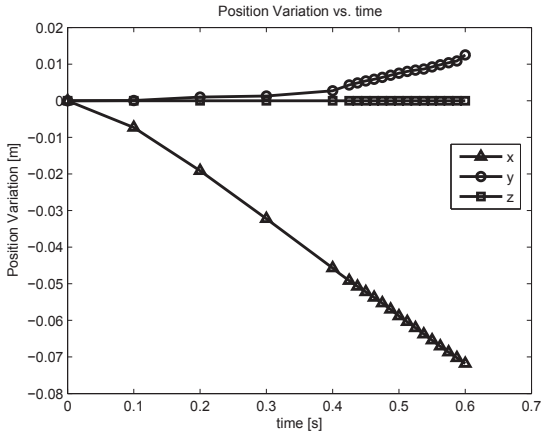

Figure 3.12: Position variation components (x, y, z) of the particle against time in the lid-driven cavity flow.

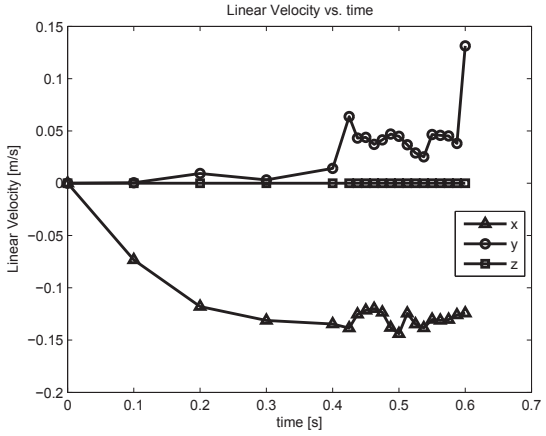

Figure 3.13: Linear velocity components (x, y, z) of the particle against time in the lid-driven cavity flow.

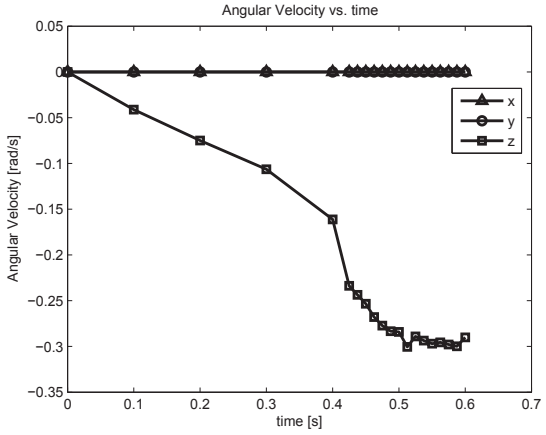

Figure 3.14: Angular velocity components (x, y, z) of the particle against time in the lid-driven cavity flow.